ORIFICE RESISTANCE FOR EJECTION INTO A GRAZING FLOW

Kenneth J. Baumeister
NASA Lewis Research Center

SUMMARY

Experiments have shown that the resistance for ejection from an orifice into a grazing flow can be less than for the no-flow case over a range of orifice velocities. To explain this decrease in orifice resistance with the addition of grazing flow, the flow from the orifice was modeled by using the inviscid analysis of Goldstein and Braun, which is valid when the orifice-flow total pressure is nearly the same as the free-stream grazing-flow total pressure. For steady outflow from an orifice into a grazing flow, the orifice flow can enter the main grazing flow in an inviscid manner without generating large eddies to dissipate the kinetic energy of the jet. From the analysis, a simple closed-form solution was developed for the steady resistance for ejection from an orifice into a grazing-flow field. The calculated resistances compare favorably with the previously published data of Rogers and Hersh in the flow regime where the total pressure difference between the grazing flow and the orifice flow is small.

INTRODUCTION

Perforated plates with back cavities are commonly used in flow ducts to dissipate acoustic energy. To predict the amount of acoustic energy absorbed by the liner, the impedance of the liner must be estimated. Either a theoretical or an empirical model is required to relate the wall impedance to the construction of the liner, the magnitude of the grazing flow, and the sound pressure level.

Many investigations of grazing-flow impedance have been performed that lead to impedance models for use in duct sound-propagation studies. Recent visual simulation studies (ref. 1) have revealed the basic physical flow process that occurs at the orifice in the presence of grazing flow. These visual studies have led to both empirical (ref. 2) and theoretical (refs. 3 and 4) impedance models both without and with grazing flow.

The theoretical studies of references 3 and 4 predict the resistance and reactance for oscillatory flow into an orifice. As yet, however, no theoretical model has been proposed for that portion of the oscillatory flow cycle where fluid is ejected from the orifice into the grazing-flow field. For steady orifice flows in the presence of a grazing flow, reference 2 presents an expression for the steady orifice resistance for small inflows or outflows. The present study develops a potential flow model for predicting the resistance of

an orifice during steady outflow in the presence of grazing flow. A simple closed-form solution is presented, and the calculated resistances are compared with measured values for the case where the total pressures of the orifice and main grazing flows are nearly the same.

SYMBOLS

C_D	discharge coefficient
c	speed of sound
d	width of orifice
H	width of channel, fig. 2
h	width of orifice jet at infinity, fig. 2
M_∞	grazing-flow Mach number, v_∞/c
P_c	total chamber pressure
P_∞	total grazing-flow pressure
p_∞	static grazing-flow pressure
S_e	slip factor
v_e^+	jet velocity upstream
v_e^-	grazing-flow velocity upstream
$\overline{v}_{jet}$	average jet velocity equal to total flow rate divided by actual area of hole
v_∞	grazing-flow velocity
z	impedance
δ	boundary-layer thickness
ϵ	total pressure difference parameter, eq. (8)
θ	steady orifice specific resistance
θ_p	steady orifice specific resistance predicted by inviscid flow theory
ρ	density

STEADY FLOW MODELS

Zorumski and Parrot (ref. 5) found for thin perforated plates that the instantaneous acoustic orifice resistance without a grazing flow is equivalent to the flow resistance of the orifice. The flow resistance is defined as the ratio of the steady pressure drop across a material to the steady velocity through the material. Feder and Dean (ref. 6) also show a close correspondence between the acoustic and steady flow resistances in the presence of a grazing flow.

Figure 1 shows, schematically, typical steady resistance data for airflow through an orifice both with and without a grazing airflow. The symmetrical straight lines represent resistance for flow into and out of the orifice with no grazing flow. Without grazing flow, vortex rings form at the orifice lip (see insert photographs in fig. 1). For either inflow or outflow with no grazing flow, nearly all the kinetic energy of the jet passing through the orifice is lost. In this simple case the resistance θ can be correlated by considering the one-dimensional energy equation (ref. 2)

$$\theta \equiv \frac{P_c - p_\infty}{\rho c \overline{v}_{jet}} = \frac{1}{2c} \frac{\overline{v}_{jet}}{C_D^2} \tag{1}$$

where the symbols are defined in the preceding section. The discharge coefficient C_D is equal to the actual area of the flow divided by the area of the hole.

In the more general case with grazing flow, the kinetic energy of the jet (assumed to be equivalent to the instantaneous acoustic energy from ref. 5) will be dissipated into heat by friction or transferred back into the mean flow field through the interaction between the jet and the grazing flow.

POTENTIAL OUTFLOW MODEL

Experiments (ref. 2) have shown that the steady outflow resistance of an orifice with grazing flow can be less than for the no-flow case over a range of orifice velocities. This is shown in figure 1 by the schematic representation of the steady orifice resistance as a function of the jet velocity and the grazing-flow Mach number. As shown in the lower left photograph of figure 1, the resistance is less with grazing than without grazing flow.

The photographic inserts in figure 1 indicate the nature of the flow fields. As reported in reference 1, dyes were injected in the vicinity of the orifice and the motion of the fluid (water) was observed. As shown in the upper left photograph of figure 1, for no grazing flow, ejection from the orifice forms large eddies around the exit lip of the orifice, resulting in the dissipation of the kinetic energy of the jet. On the other hand, with ejection from the orifice into a grazing flow, the lower left photograph in figure 1 shows much smoother flow patterns. The flow leaves the orifice, is turned by the grazing flow, and blends in with the grazing flow.

With the sharp-edge orifice under consideration here, some separation and associated vorticity are generated immediately downstream of the orifice. However, under the condition where the total pressure of the jet and the total pressure of the grazing flow are equal, the orifice flow can enter the main grazing flow in a nearly inviscid manner (refs. 7 to 9) without the generation of large eddies to dissipate the kinetic energy of the jet. Therefore, the flow from the orifice is now modeled by using the steady inviscid analysis of Goldstein and Braun (refs. 7 and 8), which is valid when the orifice-flow total pressure is nearly the same as the free-stream grazing-flow total pressure.

To determine the specific orifice steady flow resistance as defined in equation (1), the relation between the driving pressure difference ΔP and the average jet velocity $\bar{v}_{jet}$ must be determined. This relation was estimated based on an inviscid flow model shown pictorially in figure 2.

The one-dimensional continuity equations can be written across the two cell boundaries as shown in figure 2

$$v_\infty H = v_e^-(H - h) \qquad \text{(Negative domain)} \tag{2}$$

$$\bar{v}_{jet}\, d = v_e^+ h \qquad \text{(Positive domain)} \tag{3}$$

Combining equations (2) and (3) yields

$$\bar{v}_{jet} = v_\infty \frac{H}{H-h} \frac{h}{d} \frac{v_e^+}{v_e^-} \tag{4}$$

The ratio of v_e^+ to v_e^- is defined as the slip factor S_e, and the ratio h/d is defined as the contraction ratio. These factors are estimated from the inviscid theory of reference 7, which presents a solution for the injection of an attached steady-flow inviscid jet into a moving stream. The analytical solution in reference 7 applies to a two-dimensional (slot), inviscid, incompressible jet injected into a semi-infinite moving stream. The solution uses small-perturbation theory; consequently, the solution is valid when the difference between the total pressure in the main stream is not too large. Also, losses at sharp corners, in turning, and in generating eddies have been neglected. The agreement between theory and experiment will be used to justify these simplifications.

The duct flow area is assumed to be large in comparison with the total orifice flow area, so that for a typical flow duct (such as in ref. 2, to which the theory will be compared)

$$\frac{H}{H-h} \approx 1 \qquad \frac{h}{H} \ll 1 \tag{5}$$

For this condition, the semi-infinite model of reference 7 should apply. Therefore, equation (4) becomes

$$\bar{v}_{jet} = v_\infty \frac{h}{d} S_e \tag{6}$$

By using the graphical results of figure 11(e) of reference 7, the extrapolated values of the slip factor far downstream from the orifice slot can be correlated as a function of the difference between the total pressure and the total upstream pressure, as follows:

$$S_e = \frac{v_e^+}{v_e^-} \approx \frac{v_e^+}{v_\infty} = (1 + \varepsilon)^{1/2} \tag{7}$$

where

$$\varepsilon \equiv \frac{P_c - P_\infty}{\frac{1}{2}\rho v_\infty^2} \tag{8}$$

Here, ε is a small perturbation parameter that can be legitimately varied between +0.2 and -0.2. For $\varepsilon = 0$, the slip is zero (ref. 8, eq. (4)) along the entire length of the interface between the grazing- and jet-flow streams. Thus, the generation of vorticity in a real fluid will be minimized for this condition.

By using the results of figure 9 of reference 7, the ratio of the final height of the jet to the slot width h/d can be correlated as a function of ε

$$\frac{h}{d} = 0.8\left(1 + \frac{\varepsilon}{2}\right) \tag{9}$$

Substituting equations (7) and (9) into equation (6) yields

$$\bar{v}_{jet} = 0.8\, v_\infty \left(1 + \frac{\varepsilon}{2}\right)(1 + \varepsilon)^{1/2} \tag{10}$$

Since the analysis performed in reference 7 is valid for only a first-order power of ε, equation (10) can be simplified to

$$\bar{v}_{jet} \approx 0.8\, v_\infty\left(1 + \frac{\varepsilon}{2}\right)\left(1 + \frac{\varepsilon}{2}\right) \approx 0.8\, v_\infty\left(1 + \varepsilon\right) \tag{11}$$

Recall that the steady orifice resistance is defined as the ratio of the pressure difference $P_c - p_\infty$ to the jet velocity $\bar{v}_{jet}$. Since the relation of total to static pressure is defined as

$$P_\infty = p_\infty + \frac{1}{2}\rho v_\infty^2 \tag{12}$$

it follows that

$$\theta = \frac{P_c - p_\infty}{\rho c \bar{v}_{jet}} = \frac{P_c - P_\infty + \frac{1}{2}\rho v_\infty^2}{\rho c \bar{v}_{jet}} \tag{13}$$

From the definition of ε, equation (8), the specific orifice steady-flow resistance can also be written as

$$\theta = \frac{v_\infty^2\,(\varepsilon + 1)}{2c\bar{v}_{jet}} \tag{14}$$

Substituting the expression for $\bar{v}_{jet}$ from equation (11) yields

$$\theta_p = \frac{M_\infty}{1.6} \tag{15}$$

where M_∞ is the Mach number of the grazing flow upstream of the orifice, assuming a uniform flow in the duct. Equation (15) cannot be applied to the zero-grazing-flow case since the assumed flow model does not apply. The subscript p has been added to θ to indicate that this resistance has been evaluated by using a potential flow model. Significantly, the resistance θ_p is only a function of the grazing-flow Mach number and is independent of ε in this linearized theory.

The theoretical equation (15) is based on an inviscid model for which no boundary layer exists up- or downstream of the orifice. In the next section this model is compared with the data of Rogers and Hersh (ref. 2) in which the ratio of boundary-layer thickness δ, to orifice hole diameter is less than 1 ($\delta/d = 0.71$). A word of caution is necessary; for actual inlets with large δ/d, a correction for boundary-layer thickness would most likely be required. For example, for a δ/d of 4.09, the data of reference 2 show that the acoustic resistance could increase from 5 to 25 percent depending on the ratio of jet to grazing (mean) flow velocity. For applications of equation (15) to large δ/d ratios, it is suggested, therefore, that an empirical correction factor be used based on data such as those presented in reference 2.

Equation (15) is a theoretical expression for the resistance of an orifice to steady outflow. Equation (15) is a priori limited to small ε, that is, small differences between the cavity and free-stream total pressures. However, as shown in the next section, the theory does fortuitously seem to correlate the data for negative values of ε. As shown in figure 3, the close proximity of the wall prevents wave growth and thereby reduces the losses of the jet, making inviscid theory more appropriate. For large positive pressure differences (positive ε), as shown in figure 3, eddies form at the interface between the jet and the stream. Obviously, the flow cannot be assumed inviscid in this case.

EXPERIMENTAL COMPARISON

The expression for the specific orifice resistance θ_p given by equation (15) is now compared with the measured airflow data from reference 2.

Case a: Jet- and Grazing-Flow Total Pressures Equal ($\varepsilon = 0$)

The theory is first compared to the experimental data for $\varepsilon = 0$. In this case, the slip along the streamline separating the jet and grazing flow is zero; thus, vorticity generation should be at a minimum. Therefore, the inviscid theory would be best applied for this case. As seen in figure 4, the simple inviscid theory for the orifice resistance gives excellent agreement with experiment over the range of grazing-flow Mach numbers tested in reference 2.

Case b: $\varepsilon > 0$

The theory is now compared to the data of reference 2 for a range of ε. For large ε, the jet will interact with the grazing flow and generate waves and associated vorticity at the interface. Inviscid theory should not be expected to work in this range. As seen in figure 5, for the $\varepsilon > 0$ points on the data curves, the deviation between theory and experiment increases with ε.

Case c: $\varepsilon < 0$

For the case where the chamber pressure is less than the free-stream total pressure ($\varepsilon < 0$), the flow from the orifice is observed to be a smooth thin flow with no visible wave growth along the interface. The close proximity of the wall to the jet–grazing-flow interface reduces the growth rate of the waves. Reducing wave amplitude (ref. 9, p. 83) reduces the rate at which the energy of the jet is dissipated. This could explain why the inviscid theory and experiment still agree (which may be fortuitous) for large negative values of ε, as shown in figure 5.

DISCUSSION OF RESULTS

The acoustic flow resistance at a suppressor wall can be related to a transfer of acoustic energy across the boundary of the duct. Normally, the acoustic energy lost by the suppressor is assumed to be dissipated into heat inside or in the near field of the absorber. In this paper, an inviscid flow model is used to predict the steady orifice-flow resistance for ejection from an orifice into a grazing flow. This inviscid flow resistance is commonly used as part of the resistive component of the wall impedance in an acoustic suppressor analysis. How can an inviscid (frictionless) flow resistance account for the energy dissipation associated with the acoustic resistance?

A possible explanation is that the steady outflow resistance into a grazing flow is not related to the instantaneous acoustic resistance. However, many investigators assume that these resistances are related. An argument to support the latter assumption follows.

Acoustic energy can be dissipated (in a resonator for example), sent through some flanking path into the surrounding environment (such as through the structure), or transformed into a mean flow field. The last case is now considered in detail. In an acoustic field, the acoustic energy can be transformed directly into the mean grazing-flow field only in the presence of vorticity (eq. (1.87) of ref. 10). However, for $\varepsilon = 0$, the asymptotic value of the jet velocity leaving the orifice will be equal (ref. 7, eq. (4)) to the grazing-flow velocity. Therefore, the jet kinetic energy (usually assumed to represent the induced acoustic jet velocity) effectively becomes a part of the grazing-flow field, since the two fluids are now indistinguishable. Since the marging of the two streams occurs in an irrotational manner, the flow field in the vicinity of the orifice is not acoustic. In fact, the orifice velocities

generated by the far-field acoustic pressures can be described by the incompressible momentum equations (refs. 3 and 4).

The flow field near the wall, therefore, is termed the nonacoustic boundary region (fig. 6). The acoustic flow region is adjacent to this region, as shown in figure 6. It is commonly assumed that the pressure and velocity at the boundary of the nonacoustic region (dashed line in fig. 6) are valid boundary conditions for the region where the acoustic equations apply. The ratio of pressure to velocity at this boundary is defined as the impedance z. In addition, the steady flow resistance is assumed to be equal to the instantaneous acoustic resistance (real part of impedance).

From the preceding discussion, the interpretation of a dissipative, resistive boundary condition developed by an inviscid theory must imply that the acoustic energy is lost by a process other than frictional dissipation. In this case (fig. 6), the kinetic energy of the acoustic jet becomes part of the steady grazing flow in the nonacoustic region adjacent to the orifice. Since this transfer of energy occurs outside the acoustic field, the usual acoustic flow laws (requiring vorticity for energy transfer to a grazing flow) are not violated. Therefore, there is no conceptual problem in relating a frictionless steady flow resistance to an acoustic resistance.

In summary, sound impinging on a resonator cavity is partially reflected and partially absorbed. During the positive portion of the sound pressure cycle (with or without grazing flow), the nonreflected potential energy of the impinging pressure wave induces flow into the orifice. The kinetic energy of the induced flow is stored in the back cavity (system reactance) and partially dissipated by viscous scrubbing and flow expansion. During the negative portion of the sound pressure wave, the cavity gives up its stored energy and drives the fluid out. In the absence of grazing flow, the kinetic energy of the acoustic jet undergoes an abrupt change in flow area that leads to dissipation of its kinetic energy. With grazing flow, some of the kinetic energy of the jet can be diverted back into the grazing flow. In both cases, all the kinetic energy of the jet is lost to the acoustic field.

CONCLUSIONS

Experiments have shown that the resistance for ejection from an orifice with grazing flow can be less than for the no-flow case over a range of orifice velocities. A simple closed-form inviscid solution was shown to explain the decrease in orifice resistance with grazing flow.

REFERENCES

1. Baumeister, Kenneth J.; and Rice, Edward J.: Visual Study of the Effect of Grazing Flow on the Oscillatory Flow in a Resonator Orifice. NASA TM X-3288, 1975.

2. Rogers, T.; and Hersh, A. S.: The Effect of Grazing Flow on the Steady-State Resistance of Isolated Square-Edged Orifices. AIAA Paper 75-493, Mar. 1975.

3. Hersh, A. S.; and Rogers, T.: Fluid Mechanical Model of the Acoustic Impedance of Small Orifices. AIAA Paper 75-495, Mar. 1975.

4. Rice, Edward J.: A Theoretical Study of the Acoustic Impedance of Orifices in the Presence of a Steady Grazing Flow. NASA TM X-71903, 1976.

5. Zorumski, William E.; and Parrot, Tony L.: Nonlinear Acoustic Theory for Rigid Porous Materials. NASA TN D-6196, 1971.

6. Feder, Ernest; and Dean, Lee W., III: Analytical and Experimental Studies for Predicting Noise Attenuation in Acoustically Treated Ducts for Turbofan Engines. NASA CR-1373, 1969.

7. Goldstein, Marvin E.; and Braun, Willis: Injection of an Attached Inviscid Jet at an Oblique Angle to a Moving Stream. NASA TN D-5501, 1969.

8. Goldstein, M. E.; and Braun, Willis: Inviscid Interpenetration of Two Streams with Unequal Total Pressures. J. Fluid Mech., vol. 70, pt. 3, Aug. 1975, pp. 481-507.

9. Bird, R. B.; et al.: Lectures in Transport Phenomena. Continuing Education Series 4, Am. Inst. Chem. Engrs., 1969.

10. Goldstein, Marvin E.: Aeroacoustics. McGraw-Hill Book Co., Inc., 1976.

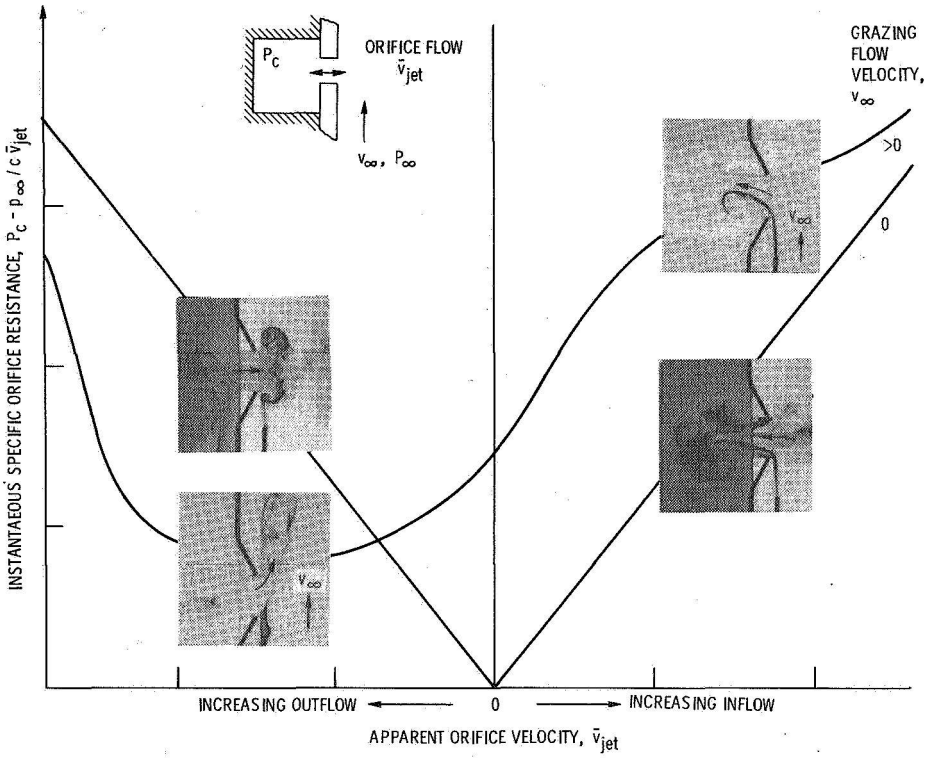

Figure 1. - Effect of sinusoidally varying orifice flow rate on instantaneous specific orifice resistance and flow profiles.

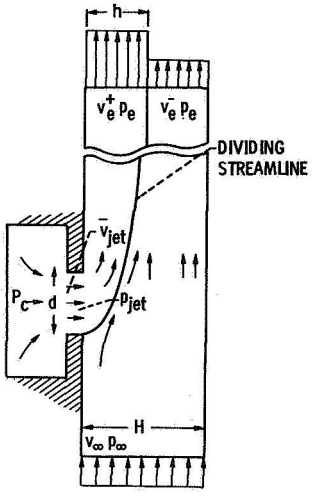

Figure 2. - Flow injection model of attached inviscid jet at right angle to moving stream.

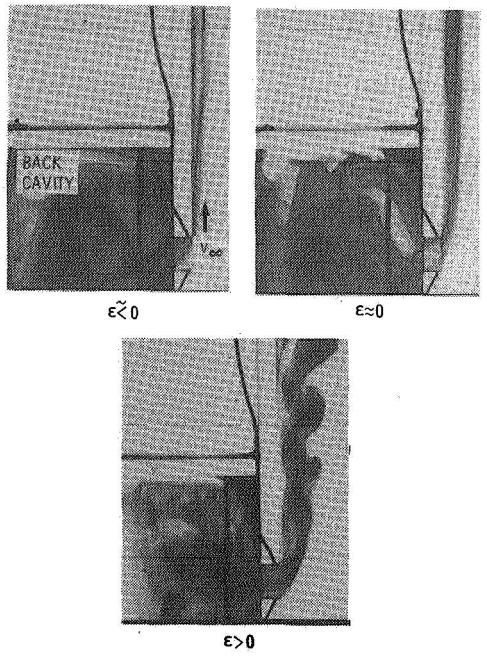

Figure 3. - Effect of increasing chamber pressure on shape of flow field.

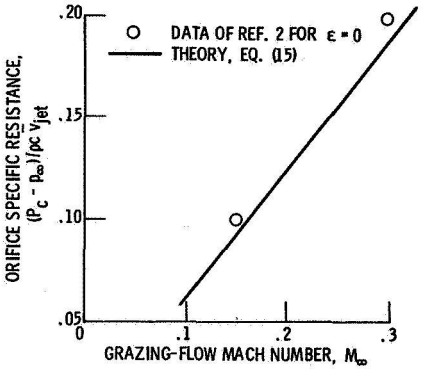

Figure 4. - Steady flow resistance as calculated from potential flow theory compared with data for total pressure difference parameter $\epsilon = 0$.

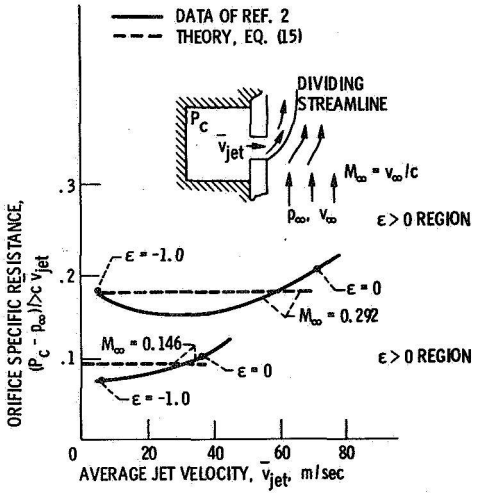

Figure 5. - Steady flow resistance as calculated from potential flow theory compared with data.

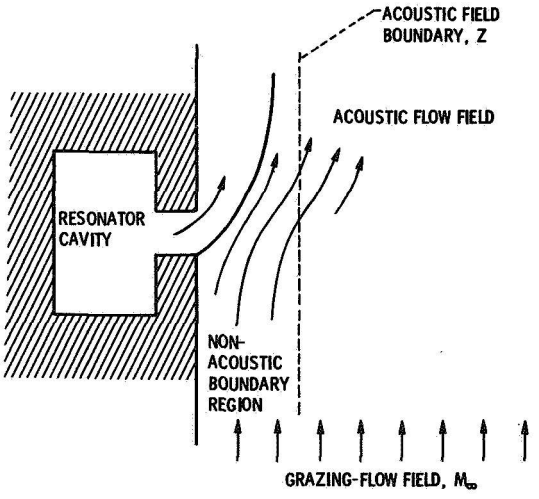

Figure 6. - Flow regimes in vicinity of orifice.